Surface relief gratings formed by microphase-separated disperse red 1 acrylate-containing diblock copolymers

Mitica Cezar Spiridon, Karim Aissou, Muhammad Mumtaz, Cyril Brochon, Eric Cloutet, Guillaume Fleury, Georges Hadziioannou

Surface Relief Gratings Formed by Microphase-Separated Disperse Red 1 Acrylate-Containing Diblock Copolymers

Mitica Cezar Spiridon,[1] Karim Aissou,[1*] Muhammad Mumtaz,[1] Cyril Brochon,[1] Eric Cloutet,[1] Guillaume Fleury[1*] and Georges Hadziioannou[1]

[1]Laboratoire de Chimie des Polymères Organiques (LCPO), CNRS UMR 5629 - ENSCPB - Université de Bordeaux, 16 Avenue Pey-Berland, F-33607 Pessac Cedex, France

E-mail: karim.aissou@enscbp.fr, gfleury@enscbp.fr

Keywords: ATRP, block copolymer, surface-relief grating, self-assembly.

Abstract:

Sinusoidal surface-relief gratings (SRGs) formed by micro-phase separated photoresponsive polydimethylsiloxane-*block*-poly(methyl acrylate)-*co*-poly(disperse red 1 acrylate) (PDMS-*b*-P(MA-*co*-DR1A)) chains are investigated. Different PDMS-*b*-P(MA-*co*-DR1A) were prepared by a multi-step synthetic approach which overcomes the challenges inherent to the synthesis of well-defined PDMS-based block copolymers (BCPs) having a DR1A dye content up to 50 wt%. A sinusoidal SRG (amplitude ≈ 5 nm, wavenumber ≈ 315 nm) interferometrically inscribed onto a thin PDMS-*b*-P(MA-*co*-DR1A) layer exhibiting an out-of-plane cylindrical structure with a period of ~34 nm is demonstrated. Such kind of "two-colored" multiscale patterned surfaces could be envisioned as guiding patterns to efficiently direct the self-assembly of a BCP upper-layer *via* a hybrid chemo-/grapho-epitaxial alignment of BCP features.

Photoresponsive materials combining an efficient surface-relief grating (SRG) formation and a microphase-separation at the nanometer scale are attractive materials to produce advanced surfaces with hierarchical multiscale functionalities which are highly-desired for holography storage and next-generation lithography [1]. For instance, phase-type holographic materials with an improved diffraction efficiency have been demonstrated from SRGs formed by microphase-separated azobenzene-containing liquid-crystalline block copolymers (BCPs) [2]. Here the high diffraction efficiency, arising from the formation of both a SRG and a refractive-index grating, makes such holographic materials promising candidates for storage of high-density information, as well as for recording three dimensional objects. In another example, the practicable control of the direction of a azobenzene containing block copolymer structure was established using linearly polarized light [3,4]. The inscription of SRG patterns in such block copolymer layer provides an additional lever to control the block copolymer structure orientation through the thickness modulation resulting from the SRG patterning [5]. The directed self-assembly (DSA) of BCPs into laterally-ordered sub-10 nm features (*i.e*. cylinders or lamellae) with an out-of-plane orientation are highly-desired for the next-generation lithography [6–10]. So far, such control of the lateral-order of features is achieved by either graphoepitaxy [6,11–13] or chemoepitaxy patterns [14]. As both chemical and topographical patterns with a modulation of the surface energy and the height amplitude of the polymeric layers can be achieved from microphase-separated azobenzene-containing BCPs, such photoactive materials can be also envisioned as efficient guiding patterns to direct the self-assembly of BCP features.

In this communication, we explore the potential of block copolymers containing azobenzene moieties as directed self-assembly methodology for the formation of multiscale patterned surfaces through SRG formation combined to BCP self-assembly. A poly(dimethylsiloxane)-*b*-poly(methyl acrylate-*co*-disperse red 1 acrylate) (PDMS-b-P(MA-

co-DR1A)) system was synthetically designed for this purpose as the association of a low glass transition temperature PDMS block to the photostimulable P(MA-co-DR1A) block is expected to facilitate the mass transfer resulting from the SRG inscription. The study of the self-assembly, both in bulk and in thin film configuration, was performed by Small Angle X-ray Scattering (SAXS) and Atomic Force Microscopy (AFM) techniques in order to study the nanoscale phase separation provided through the chemical incompatibility of the blocks. Topographical and chemical patterns were subsequently produced by exploiting the self-assembly of BCP chains consisting of the azobenzene block, for efficient production of photo-induced surface patterns (*i.e.* graphoepitaxy), associated to a Si-containing block which forms features on the sinusoidal surface-relief gratings, and so acting as periodic nanoscale chemical patterns (*i.e.* chemoepitaxy).

The photoactive BCP system, namely poly(dimethylsiloxane)-*b*-poly(methyl acrylate-co-disperse red 1 acrylate), was obtained by combining a well-defined PDMS-macro initiator block to a disperse red 1 (DR1) moieties embedded along the side-chain of a polyacrylate-type block. The embedment of a DR1 dye in the side-chain of a BCP architecture demands careful consideration of the synthetic pathway. Indeed the synthesis of DR1 containing polymers is rather difficult due to the inhibition effect of the DR1 monomers towards active centers such as radicals. As an additional constraint, a sufficient amount of photo-active moieties has to be incorporated in order to allow the SRG formation (ca. 30 wt% of azo-dye) [15]. DR1 type azobenzene dyes can be embedded in the side-chain of polymers by (co)polymerization of DR1 containing monomers [16–19] or via polymer-analogous reactions [20,21]. DR1 monomers, such as DR1 (metha)acrylate [17,18], are usually polymerized in an uncontrolled fashion by classical free radical polymerization. For instance, the ATRP of DR1 (metha)acrylate type monomers is not well controlled due to the catalyst complexation [22]. The RAFT copolymerization of DR1 (metha)acrylate type monomers offers a better control of the

polymerization [23] but limits the amount of the embedded dye in the final polymer which is consequently not sufficient to induce the SRG formation [24,25]. In this context, polymer-analogous reactions of DR1 with a predefined BCP was preferred to obtain well-defined BCP structures with adequate DR1 content [26,27].

Living anionic polymerization was chosen for the synthesis of well-defined PDMS blocks as such methodologies allow to subsequently use the PDMS chains as macro-initiators [28] in the GTP [29], RAFT [30], ATRP [31] of specific monomers or in coupling methods [32] such as click chemistry [33]. The incorporation of the DR1 moiety in the PDMS-based BCP was obtained from a poly(dimethylsiloxane)-b-poly(methyl acrylate-co-acrylic acid) precursor through esterification with the carboxylic acid groups [20,34,35]. A poly(dimethylsiloxane)-b-poly(methyl acrylate-co-tert-butyl acrylate) architecture was used as intermediate since direct copolymerization of acrylic acid and methyl acrylate is unsuitable [36–38]. Finally an appropriate deprotection step generates the carboxylic acid groups required for the esterification of DR1 moieties along the BCP chains. Hence the synthesis approach of the novel BCP architecture consists of three main steps: (i) the synthesis of poly(dimethylsiloxane)-b-poly(methyl acrylate-co-tert-butyl acrylate) *via* anionic polymerization and ATRP, (ii) the controlled deprotection of the tert-butyl acrylate units and, (iii) the esterification reaction with DR1; as presented in Scheme 1.

Scheme 1. Synthetic pathway used for poly(dimethylsiloxane)-b-poly(methyl acrylate-co-disperse red 1 acrylate).

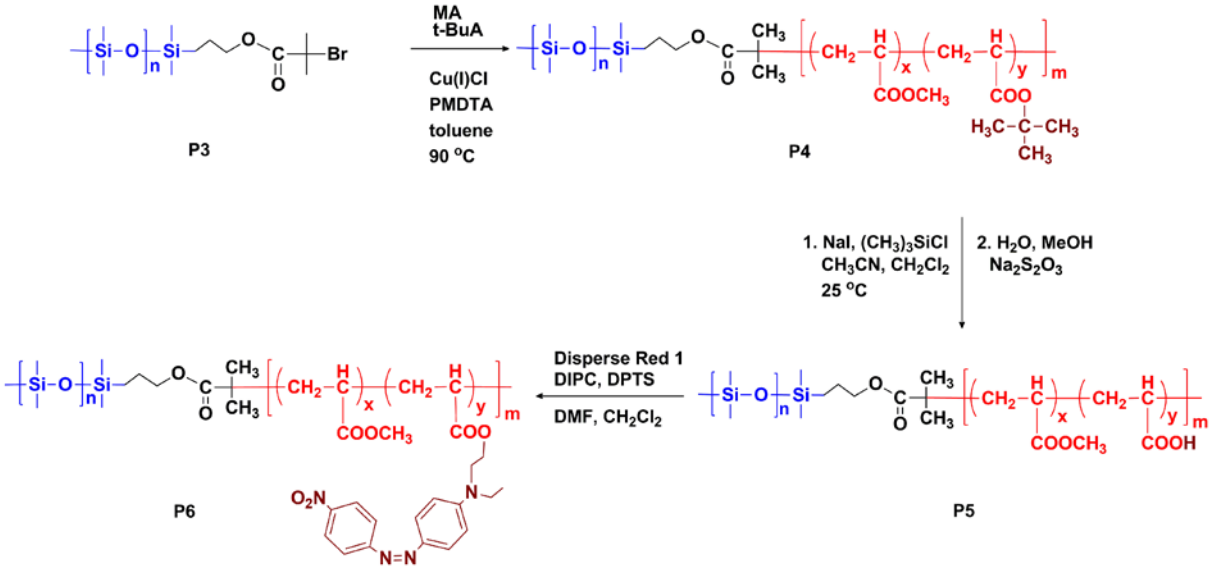

Synthesis of poly(dimethylsiloxane)-b-poly(methyl acrylate-co-tert-butyl acrylate).

In the first step, a poly(dimethylsiloxane)-*b*-poly(methyl acrylate-*co*-tert-butyl acrylate) (P4) was obtained by ATRP using a mono-2-bromoisobutyrate terminated PDMS macro-initiator (P3) as 2-bromoisobutyrates are efficient initiators for the ATRP of (metha)acrylates [39]. To prepare this macro-initiator, a living PDMS was obtained first by anionic polymerization of hexamethylcyclotrisiloxane (D3), as described in Supporting Information. The initiation of D3 polymerization by sec-butyl lithium was accomplished in cyclohexane at 30°C followed by the addition of THF after 3 hours to promote the polymerization. The reaction was terminated after another 4 hours with chlorodimethylsilane prior to full monomer conversion. In this fashion, undesirable side reactions like backbiting and redistribution are avoided. Two mono-hydride terminated PDMS (P1-a and P1-b) were synthesized following this synthetic pathway with molecular weight close to 10 kg/mol according to the end-group analysis given by ^{1}H-NMR (see Figure S1). The $(CH_3)_2SiH$ chain-end functionality of P1-a and P1-b is close to unity, as determined by comparison of the integration of the methine proton of sec-butyl groups at 0.54 ppm and the hydrosilyl proton at 4.7 ppm (see Figure S1).

The hydrosilylation reaction of the $(CH_3)_2SiH$ end-groups and allyl alcohol was mediated by Karstedt's catalyst to obtain mono-carbinol terminated PDMS precursors (P2), as described in Supporting Information. The chain-end functionality for both P2-a and P2-b was determined to be ca. 0.9, through the comparison of the integration for the methine proton of sec-butyl groups overlapped with Si-CH_2- protons at 0.55 ppm and for the -CH_2- protons next to -OH at 3.6 ppm (see Figure S2). The synthesized mono-carbinol PDMS were finally transformed into ATRP macro-initiators (P3-a and P3-b) after the acylation with 2-bromoisobutyryl bromide (see Supporting Information). The conversion is quantitative and ^{1}H-NMR characterization confirms a chain-end functionality of ca. 0.9 for both P3-a and P3-b polymers (see Figure S3). The value of the Mn and the polydispersity index for both P3 polymers remains almost unchanged as regards to the P2 precursors (see Table 1).

Table 1. Macromolecular characteristics of the synthesized polymers

Polymers	Theoretical Mn kg/mol	Mn (^{1}H-NMR) kg/mol	Mn (SEC)[a] kg/mol	Đ	Composition[b] (wt%)
2a	12.4	10.8	11.9	1.12	n.a.[c]
2b	12.3	9.6	9.7	1.07	n.a.[c]
3a	12.4	10.3	11.5	1.08	n.a.[c]
3b	12.3	10.4	10.1	1.08	n.a.[c]
4a	18.1	16.9	22.2	1.21	*DMS/tBA/MA* 61/26/13
4b	24.9	26.7	22.4	1.22	*DMS/tBA/MA* 39/43/18
5a	14.9	15.2	n.d.[d]	n.d.[d]	*DMS/tBA/MA/AA* 68/3/14/15
5b	21.6	22.4	n.d.[d]	n.d.[d]	*DMS/tBA/MA/AA* 46/8/21/25
6a	24.2	25.7	19.2	1.35	*DMS/tBA/MA/DR1A* 40/2/9/49
6b	45.1	30.9	29.7	1.22	*DMS/tBA/MA/DR1A* 34/6/15/45

[a] determined by SEC in THF at 40°C using the PS standards. [b] determined using ^{1}H-NMR. [c] non applicable. [d] non determined due to the strong interaction between the stationary phase of the SEC columns and the BCPs in THF.

Methyl acrylate (MA) and tert-butyl acrylate (tBA) were successfully copolymerized by ATRP using the synthesized PDMS macro-initiators, as presented in Scheme 1 (see Supporting Information for experimental details). A mixed halogen initiation system was used considering the high propagation rate constants for (meth)acrylates polymerizations [40,41]. The halogen exchange occurs rapidly at the set temperature and the exchange of the bromine by the chlorine atom diminishes undesirable secondary reactions (which originate from the more labile carbon-bromine bond) by decreasing the radical concentration.

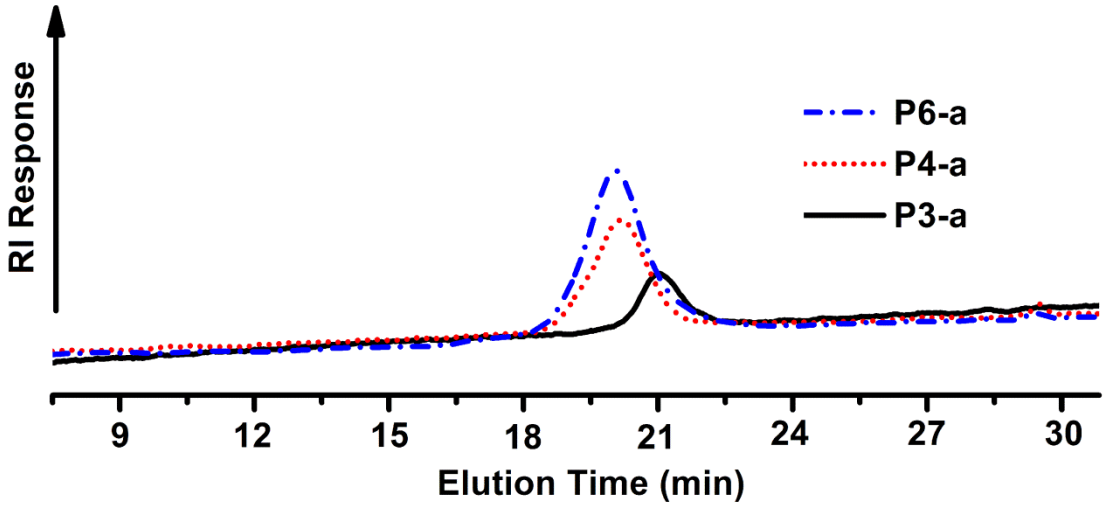

Figure 1. Overlaid SEC traces (THF, 40°C, trichlorobenzene (TCB) as flow marker) of the macro-initiator P3-a, the corresponding diblock copolymer P4-a and the azo-copolymer P6-a.

As shown in Figure 1, the SEC trace of the P4-a BCP appears clearly shifted as regards to the P3-a PDMS macro-initiator highlighting the successful copolymerization of the second block from the ATRP macro-initiator. The absence of a shoulder at higher retention times proves the high efficiency of the initiation system. The Mn value obtained by SEC analysis using polystyrene standards are close to the expected one and the BCP composition is in accordance with the initial feed ratio as determined by ^{1}H-NMR (Figure S4). Table 1

summarized the macromolecular characteristics of the synthesized BCPs. The results obtained from differential scanning calorimetry (DSC) confirm the synthesis of segregated diblock copolymers with the presence of the characteristic thermal transitions of each block, i.e. the PDMS melting temperature at -41°C and the glass transition of the P(tBA-*co*-MA) block at 28°C (see Figure S5). Incorporation of tBA moieties was further evidence by a large endothermic peak at ca. 210°C assigned to the evaporation of isobutylene formed from the decomposition of the tBA groups [42].

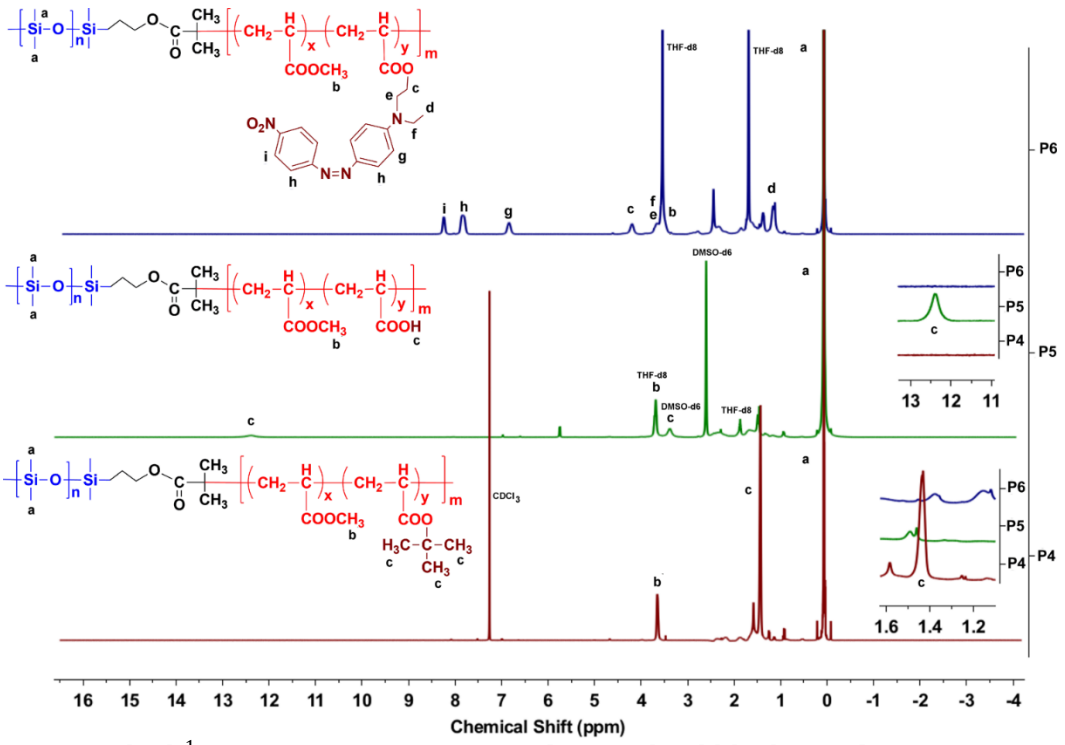

Figure 2. Overlaid ^{1}H-NMR spectra corresponding to the diblock copolymers: P4 in $CDCl_3$, P5 in a mixture of THF-d8 and DMSO-d6, and P6 in THF-d8.

Synthesis of poly(dimethylsiloxane)-b-poly(methyl acrylate-co-disperse red 1 acrylate).

The synthesis of the dye-containing BCPs requires a deprotection approach which does affect neither the acid- and base-sensitive PDMS backbone [43], nor the ester linkage between the two blocks. Preliminary tests using $ZnBr_2$ as deprotecting reagent (see Supporting Information) prove to be suitable for the hydrolysis of the t-butyl ester moieties but also lead to some cleavage of the ester bond between the two blocks. As opposed, in situ generated

trimethylsilyl iodide (TMSI) allows the dealkylation of the t-butyl ester groups yielding the corresponding silyl ester groups [44,45] which were subsequently hydrolyzed in a water/methanol mixture to carboxylic acid (see Supporting Information for experimental details). ^{1}H-NMR analysis (see Figure 2) confirms the hydrolysis of the t-butyl ester groups with no influence of both the PDMS block and the ester linkage between the two blocks. The composition of the P5 copolymers was determined by 1H-NMR (see Figure S6) resulting in DMS/tBA/MA/AA weight fractions (wt%) of 68/3/14/15 for P5-a and 46/8/21/25 for P5-b, confirming a mostly quantitative chemical deprotection of tBA moieties. The successful hydrolysis of P4 copolymers is also reflected on the DSC thermograms by the shift of the glass transition of the second block from 28°C for the P(tBA-co-MA) block in P4-a to 86°C for the P(AA-co-MA) block in P5-a (see Figure S5). It is noteworthy that the large endothermic peak related to the thermal decomposition of tBA moieties apparent on the P4 copolymers DSC thermograms is not present for the P5 copolymers, underlining the successful deprotection to a large extent.

The embedding of DR1 in the side-chain of the block copolymer P5 was performed using a modified Steglich esterification method which employs N,N′-diisopropylcarbodiimide (DIPC) and 4-(dimethylamino)pyridinium p-toluenesulfonate (DPTS) as catalysts (see Scheme 1 and Supporting Information for experimental details). Interestingly it was found that this 1:1 molecular complex between DMAP and pTSA was more effective than DMAP alone in order to yield a higher loading of the dye [46]. The attachment of the dye was confirmed by the appearance of a signal at 4.24 ppm in the ^{1}H-NMR spectrum of the P6 copolymers (see Figure 2) assigned to the oxymethylene protons of the ester linkage between DR1 and P5. The composition of the P6 copolymers was determined by ^{1}H-NMR (see Figure S7) resulting in DMS/tBA/MA/DR1A weight fractions (wt%) of 40/2/9/49 for P6-a and 34/6/15/45 for P6-b.

The SEC chromatograms of the P6 copolymers did not show a clear shift as regards to the parent P4 copolymers as the dye moieties strongly interacts with the stationary phase of the GPC columns. As an indirect evidence of the formation of well-defined block copolymers through this synthetic pathway, DOSY-NMR analysis shows only one room-temperature diffusion coefficient in THF-d8 for P6 copolymers and confirms the absence of impurities such as the PDMS macro-initiator (see Figure S8 and S9). No drastic modifications of the DSC thermograms of P6 copolymers were noticed apart a small shift of the glass transition temperature of the P(MA-co-DR1A) block at 86°C (see Figure S5). UV-Vis absorption spectroscopy measurements of P6 copolymers performed in THF at 25°C show the characteristic absorptions of DR1 moieties; i.e. a maximum at 285 nm which is attributed to the π–π* transitions of the aromatic rings, and a strong absorption band at 470 nm which corresponds to the n-π* transitions of nitrogen lone pairs (see Figure S10) [47].

Self-assembly behavior of poly(dimethylsiloxane)-b-poly(methyl acrylate-co-disperse red 1 acrylate).

Synchrotron small angle X-ray scattering (SAXS) patterns of the P6-a and P6-b samples are presented in Figure 3. The SAXS pattern of the bulk P6-a sample presents a first-order peak, q^*, at 0.186 nm^{-1} and higher-order peaks located at q/q^* = 1, 2, 3, 4 and 6, consistent with a lamellar phase having a period, *p*, of ~34.5 nm. Such morphological assignment is in accordance with the BCP composition taking into account the higher density of the (methyl acrylate-*co*-disperse red 1 acrylate) block. Atomic force microscopy (AFM) image presented in Figure 3b shows a solvent-annealed (3h, THF) P6-a thin film (p ~ 32 nm) treated by a CF_4/O_2 reactive ion etching (RIE) plasma to remove the PDMS surface wetting layer, in which an out-of-plane lamellar structure can be observed. The lamellar pitch measured from AFM is slightly smaller than the bulk periodicity obtained by SAXS. The poorly-defined SAXS pattern of the

bulk P6-b sample could be tentatively assigned to a hexagonal-close packed (HCP) cylindrical structure with a period, *p*, of ~35.8 nm (*p*6*mm* symmetry) with few peaks located at $q/q^* = 1$, $3^{1/2}$, $4^{1/2}$ and $7^{1/2}$ ($q^* = 0.2$ nm^{-1}). Here the bulk period is in accordance with the pitch measured from a solvent-annealed (3h, THF) P6-b thin film exhibiting both in-plane and out-of-plane cylinder orientations ($p \sim 34.5$ nm) (see Figure 3).

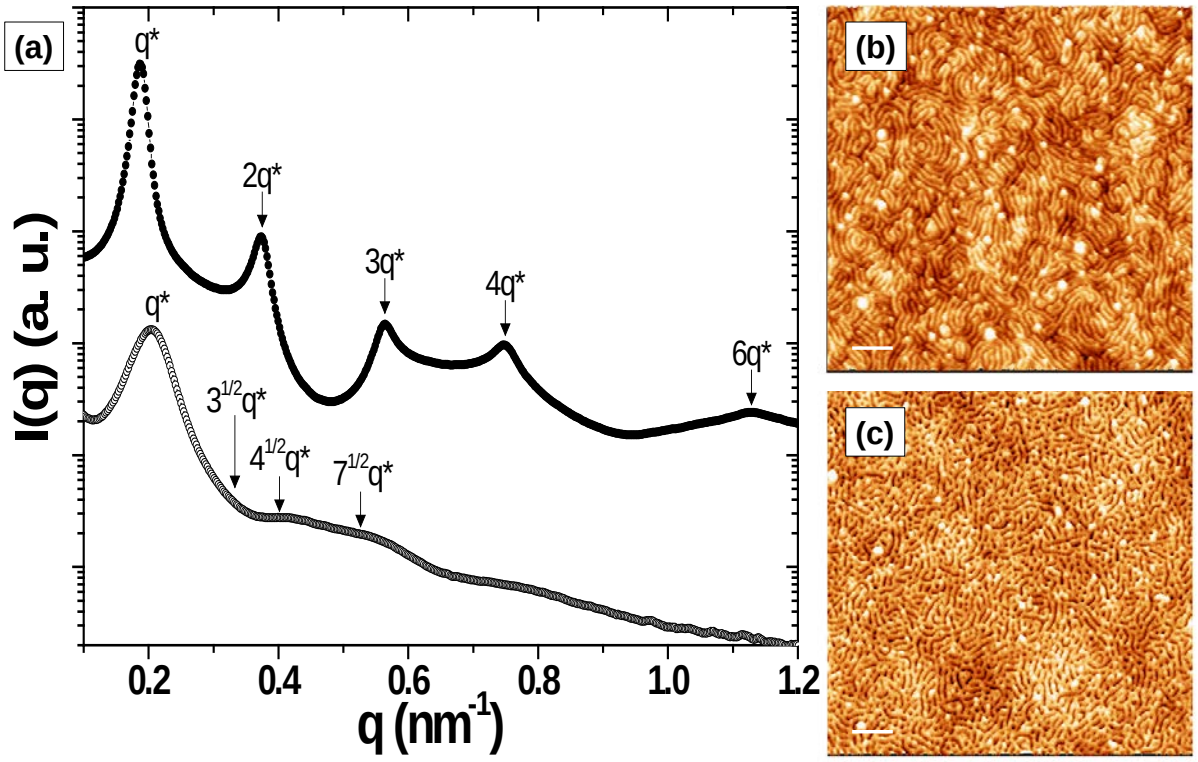

Figure 3. (a) Synchrotron SAXS patterns of the lamellar PDMS-b-P(MA-co-DR1A) P6-a (full dots) and cylindrical PDMS-b-P(MA-co-DR1A) P6-b (empty dots) samples obtained at room temperature (Curves have been shifted vertically for clarity). (b) and (c) AFM topographic views of solvent-annealed (3h, THF) lamellar PDMS-b-P(MA-co-DR1A) P6-a and cylindrical PDMS-b-P(MA-co-DR1A) P6-b thin films, respectively, treated by a CF4/O2 RIE plasma. Scale bars: 200 nm.

To inscribe a sinusoidal pattern on the microphase separated azobenzene-containing BCP layer surface, the photo-induced motion property of azobenzene groups was exploited to generate the surface-relief grating (SRG) by using a Lloyd's mirror interferometer set up [13]. The 3D-AFM topographic image presented in Figure 4a-b shows the formation of a sinusoidal pattern inscribed into the microphase-separated 180 nm thick P6-a and P6-b BCP layers with a *p*-polarized laser beam ($\lambda = 532$ nm). As extracted from the height cross section profile averaged

over the *y* axis (see Figure 4c-d), the produced sinusoidal patterns have a 315 nm wave period with an amplitude of ~5 nm, independently of the exposed BCP layers. Nevertheless the quality of the sinusoidal patterns strikingly differs between the lamellar and cylindrical BCPs. While the pattern quality is reasonably good for P6-a, no segregated BCP structure is visible on the AFM view presented in Figure 4a. As opposed, the P6-b layer shows highly defective segregated BCP structure, but the overall quality of the sinusoidal pattern inscribed is poor as regards to common SRG patterns inscribed from substituted poly(methacrylate) layers [1]. This effect is amplified for the P6-b layer due to dewetting phenomenon observed during the thin film process which leads to ill-defined patterns in the dewetted regions.

The overall SRG behavior of these BCP layers, and particularly the low thickness modulation induced by the SRG inscription (~ 5nm), is inherent to the lack of mobility induced by the already segregated as-casted block copolymer thin film even if a low T_g PDMS block was associated to the P(MA-co-DR1A) block to counterbalance this effect. As a consequence a highly disrupted block copolymer structure is obtained after the SRG patterning. Subsequent attempts to improve the BCP structures for both P6-a and P6-b by either solvent or thermal annealing did not lead to conclusive results.

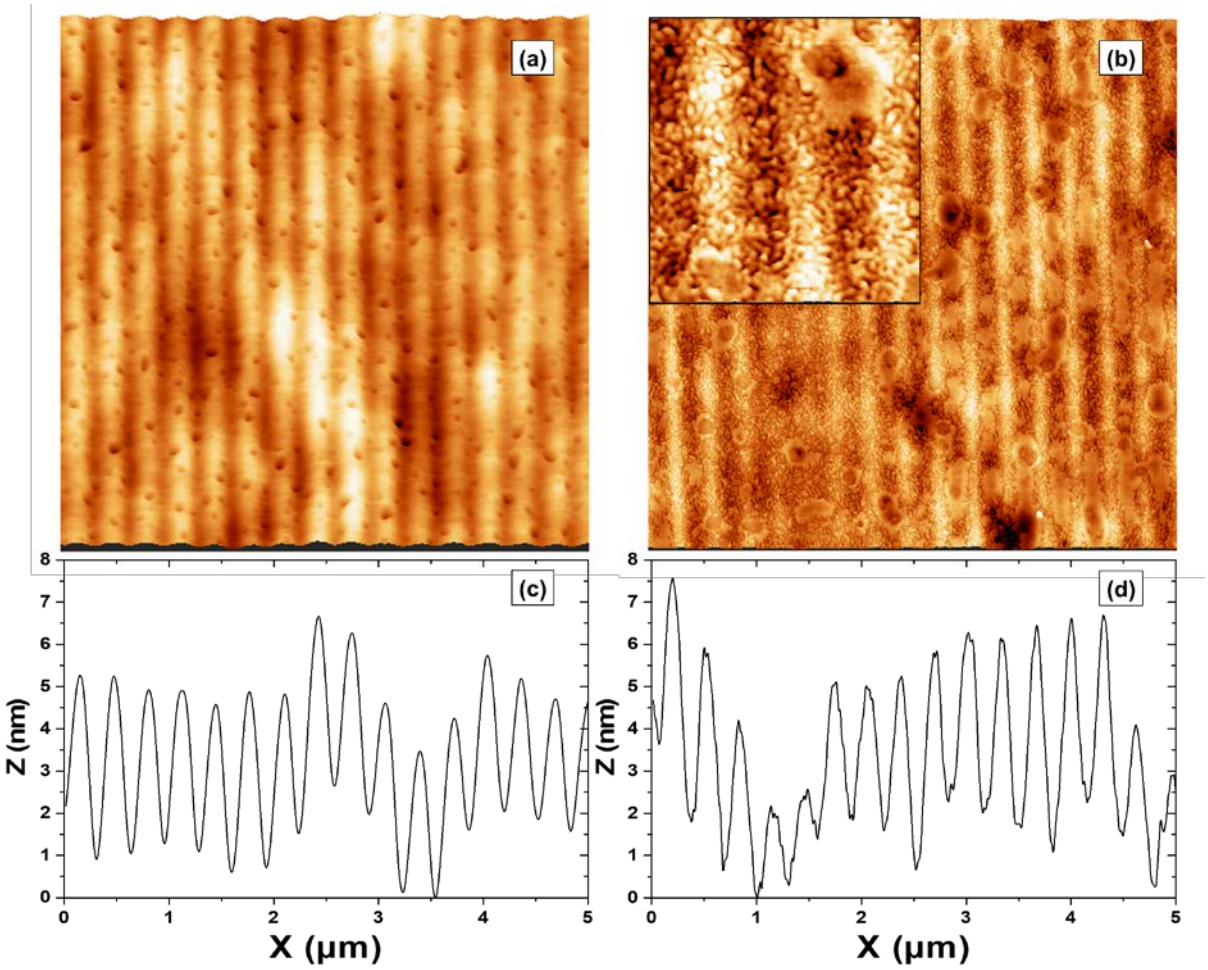

Figure 4. (a, b) (5 × 5 µm) AFM topographic views and (c, d) their associated height cross section profiles averaged over the *y* axis of solvent-annealed (3h, THF) P6-a and P6-b thin films after the sinusoidal pattern inscription into a 180 nm layer then subsequently treated by a CF_4/O_2 RIE plasma to remove the PDMS top layer.

To conclude, the employed synthetic approach is a suitable method for obtaining well-defined PDMS-based BCP containing DR1 moieties, with loadings up to 50 wt%. The embedment of larger amounts of dye has proven to be more difficult to control using the same reaction conditions. These photo-responsive materials were used to subsequently demonstrate the concept of having a PDMS-based BCP capable to exhibit both surface relief gratings and self-assembly on the surface-layer. Such sinusoidal patterns inscribed onto a microphase-separated Si-containing layer could be envisioned as guiding patterns to direct the self-assembly of high-χ BCP materials for next-generation lithography. As high-χ materials are generally Si-containing BCPs, laterally-ordered sub-10 nm features with an out-of-plane orientation could

be achieved on such advanced surfaces combining both grapho- and chemo-epitaxies. Future works targeting the improvements of the hierarchical patterning obtained from such photoactive BCP systems are currently under progress using BCP chains with enhanced mobility obtained either by the copolymerization of the DR1 methacrylate units with methacrylate units bearing longer alkyl chains (butyl or hexyl) or by the addition of plasticizing molecules into the nanostructured thin films.[48] Such methodologies are envisioned to favor the mass transfer involved during the SRG patterning, resulting thus in higher quality patterns.

Acknowledgements.

The research leading to these results has received partial funding from the PLACYD project (ENIAC Joint Undertaking program) under grant agreement #621277. The D2AM CRG Beamline is acknowledged for allocating beam time at ESRF for the SAXS experiments. This work was performed within the framework of the Equipex ELORPrintTec ANR-10-EQPX-28-01 and the LabEx AMADEUS ANR-10-LABEX-0042-AMADEUS with the help of the French state Initiative d'Excellence IdEx ANR-10-IDEX-003-02 and the ANR/Arkema industrial chair "HOMERIC" ANR-13-CHIN-0002-01.

References.

[1] H. Yu, T. Kobayashi, Photoresponsive Block Copolymers Containing Azobenzenes and Other Chromophores, Molecules. 15 (2010) 570–603. doi:10.3390/molecules15010570.

[2] H. Yu, K. Okano, A. Shishido, T. Ikeda, K. Kamata, M. Komura, T. Iyoda, Enhancement of Surface-Relief Gratings Recorded on Amphiphilic Liquid-Crystalline Diblock Copolymer by Nanoscale Phase Separation, Adv. Mater. 17 (2005) 2184–2188. doi:10.1002/adma.200500346.

[3] Y. Morikawa, T. Kondo, S. Nagano, T. Seki, Photoinduced 3D Ordering and Patterning of Microphase-Separated Nanostructure in Polystyrene-Based Block Copolymer, Chem. Mater. 19 (2007) 1540–1542. doi:10.1021/cm0630845.

[4] M. Sano, M. Hara, S. Nagano, Y. Shinohara, Y. Amemiya, T. Seki, New Aspects for the Hierarchical Cooperative Motions in Photoalignment Process of Liquid Crystalline Block Copolymer Films, Macromolecules. 48 (2015) 2217–2223. doi:10.1021/acs.macromol.5b00299.

[5] Y. Morikawa, S. Nagano, K. Watanabe, K. Kamata, T. Iyoda, T. Seki, Optical Alignment and Patterning of Nanoscale Microdomains in a Block Copolymer Thin Film, Adv. Mater. 18 (2006) 883–886. doi:10.1002/adma.200502573.

[6] S. Park, D.H. Lee, J. Xu, B. Kim, S.W. Hong, U. Jeong, T. Xu, T.P. Russell, Macroscopic 10-terabit-per-square-inch arrays from block copolymers with lateral order., Science. 323 (2009) 1030–3. doi:10.1126/science.1168108.

[7] J.W. Jeong, Y.H. Hur, H. Kim, J.M. Kim, W.I. Park, M.J. Kim, B.J. Kim, Y.S. Jung, Proximity Injection of Plasticizing Molecules to Self-Assembling Polymers for Large-Area, Ultrafast Nanopatterning in the Sub-10-nm Regime, ACS Nano. 7 (2013) 6747–6757. doi:10.1021/nn401611z.

[8] J.D. Cushen, I. Otsuka, C.M. Bates, S. Halila, S. Fort, C. Rochas, J.A. Easley, E.L. Rausch, A. Thio, R. Borsali, C.G. Willson, C.J. Ellison, Oligosaccharide/silicon-containing block copolymers with 5 nm features for lithographic applications., ACS Nano. 6 (2012) 3424–33. doi:10.1021/nn300459r.

[9] K. Aissou, M. Mumtaz, G. Fleury, G. Portale, C. Navarro, E. Cloutet, C. Brochon, C.A. Ross, G. Hadziioannou, Sub-10 nm Features Obtained from Directed Self-Assembly of Semicrystalline Polycarbosilane-Based Block Copolymer Thin Films, Adv. Mater. 27 (2015) 261–265. doi:10.1002/adma.201404077.

[10] T. Seshimo, R. Maeda, R. Odashima, Y. Takenaka, D. Kawana, K. Ohmori, T. Hayakawa, Perpendicularly oriented sub-10-nm block copolymer lamellae by atmospheric thermal annealing for one minute, Sci. Rep. 6 (2016) 19481. doi:10.1038/srep19481.

[11] R.A. Segalman, H. Yokoyama, E.J. Kramer, Graphoepitaxy of Spherical Domain Block Copolymer Films, Adv. Mater. 13 (2001) 1152–1155. doi:10.1002/1521-4095(200108)13:15<1152::AID-ADMA1152>3.0.CO;2-5.

[12] J.Y. Cheng, A.M. Mayes, C. a Ross, Nanostructure engineering by templated self-assembly of block copolymers., Nat. Mater. 3 (2004) 823–8. doi:10.1038/nmat1211.

[13] K. Aissou, J. Shaver, G. Fleury, G. Pécastaings, C. Brochon, C. Navarro, S. Grauby, J.-M. Rampnoux, S. Dilhaire, G. Hadziioannou, Nanoscale block copolymer ordering induced by visible interferometric micropatterning: a route towards large scale block copolymer 2D crystals., Adv. Mater. 25 (2013) 213–7. doi:10.1002/adma.201203254.

[14] S.O. Kim, H.H. Solak, M.P. Stoykovich, N.J. Ferrier, J.J. De Pablo, P.F. Nealey, Epitaxial self-assembly of block copolymers on lithographically defined nanopatterned substrates., Nature. 424 (2003) 411–4. doi:10.1038/nature01775.

[15] O.N. Oliveira, L. Li, J. Kumar, S.K. Tripathy, Surface-Relief Gratings on Azobenzene-Containing Films, in: Z. Sekkat, W. Knoll (Eds.), Photoreact. Org. Thin Film., Elsevier, 2002: pp. 429–486. doi:10.1016/B978-012635490-4/50015-9.

[16] A. Natansohn, P. Rochon, J. Gosselin, S. Xie, Azo polymers for reversible optical storage. 1. Poly[4’-[[2-(acryloyloxy)ethyl]ethylamino]-4-nitroazobenzene], Macromolecules. 25 (1992) 2268–2273. doi:10.1021/ma00034a031.

[17] L. Ding, T.P. Russell, A Photoactive Polymer with Azobenzene Chromophore in the Side Chains, Macromolecules. 40 (2007) 2267–2270. doi:10.1021/ma062653r.

[18] D.S. Bag, S. Alam, Synthesis and characterization of photoactive chiral copolymers of

(S)-N-(1-phenyl ethyl) methacrylamide and disperse red 1 methacrylate, J. Appl. Polym. Sci. 125 (2012) 2595–2603. doi:10.1002/app.36369.

[19] I. Steyaert, G. Vancoillie, R. Hoogenboom, K. De Clerck, S. Shiratori, H. Rahier, G. Van Assche, K. De Clerck, J. Pei, L. Gonzalez, Dye immobilization in halochromic nanofibers through blend electrospinning of a dye-containing copolymer and polyamide-6, Polym. Chem. 6 (2015) 2685–2694. doi:10.1039/C5PY00060B.

[20] D. Woo, J. Kim, M.-H. Suh, H. Zhou, S.T. Nguyen, S.-H. Lee, J.M. Torkelson, Styrene/4-hydroxystyrene random, block and gradient copolymers modified with an organic dye: Synthesis by controlled radical polymerization and characterization of electrorheological properties, Polymer (Guildf). 47 (2006) 3287–3291. doi:10.1016/j.polymer.2006.03.031.

[21] D. Wang, J. Liu, G. Ye, X. Wang, Amphiphilic block copolymers bearing strong push–pull azo chromophores: Synthesis, micelle formation and photoinduced shape deformation, Polymer (Guildf). 50 (2009) 418–427. doi:10.1016/j.polymer.2008.11.010.

[22] F.J. Pavinatto, J.Y. Barletta, R.C. Sanfelice, M.R. Cardoso, D.T. Balogh, C.R. Mendonça, O.N. Oliveira, Synthesis of azopolymers with controlled structure and photoinduced birefringence in their LB films, Polymer (Guildf). 50 (2009) 491–498. doi:10.1016/j.polymer.2008.11.043.

[23] C. Pietsch, R. Hoogenboom, U.S. Schubert, Soluble Polymeric Dual Sensor for Temperature and pH Value, Angew. Chemie Int. Ed. 48 (2009) 5653–5656. doi:10.1002/anie.200901071.

[24] Y. Vázquez, L.E. Elizalde, M.A. Nájera, G. de los Santos, J.G. Telles, Photochromic Block Copolymer Poly(styrene- *b* -azo monomer) by ATRP, Macromol. Symp. 283–284 (2009) 45–50. doi:10.1002/masy.200950907.

[25] M.C. Spiridon, F.A. Jerca, V. V. Jerca, D.M. Vuluga, D.S. Vasilescu, Novel reactive monomers bearing a push-pull azo-moiety, U.P.B. Sci. Bull., Ser. B. 76 (2014) 59–70.

[26] H.R. Allcock, R. Ravikiran, M.A. Olshavsky, Synthesis and Characterization of Hindered Polyphosphazenes via Functionalized Intermediates: Exploratory Models for Electro-optical Materials, Macromolecules. 31 (1998) 5206–5214. doi:10.1021/ma971072m.

[27] M. Faccini, M. Balakrishnan, R. Torosantucci, A. Driessen, D.N. Reinhoudt, W. Verboom, Facile Attachment of Nonlinear Optical Chromophores to Polycarbonates, Macromolecules. 41 (2008) 8320–8323. doi:10.1021/ma801875w.

[28] Y. Matsuo, R. Konno, T. Ishizone, R. Goseki, A. Hirao, Precise Synthesis of Block Polymers Composed of Three or More Blocks by Specially Designed Linking Methodologies in Conjunction with Living Anionic Polymerization System, Polymers (Basel). 5 (2013) 1012–1040. doi:10.3390/polym5031012.

[29] K.T. Lim, S.E. Webber, K.P. Johnston, Synthesis and Characterization of Poly(dimethyl siloxane)−Poly[alkyl (meth)acrylic acid] Block Copolymers, Macromolecules. 32 (1999) 2811–2815. doi:10.1021/ma981658o.

[30] T.H. Duong, C. Bressy, A. Margaillan, Well-defined diblock copolymers of poly(tert-butyldimethylsilyl methacrylate) and poly(dimethylsiloxane) synthesized by RAFT polymerization, Polymer (Guildf). 55 (2014) 39–47. doi:10.1016/j.polymer.2013.11.034.

[31] M.A. Semsarzadeh, M. Abdollahi, Atom transfer radical polymerization of styrene and methyl (meth)acrylates initiated with poly(dimethylsiloxane) macroinitiator: Synthesis and characterization of triblock copolymers, J. Appl. Polym. Sci. 123 (2012) 2423–2430. doi:10.1002/app.34794.

[32] V. Bellas, H. Iatrou, E.N. Pitsinos, N. Hadjichristidis, Heterofunctional Linking Agents

for the Synthesis of Well-Defined Block Copolymers of Dimethylsiloxane and tert -Butyl Methacrylate or 2-Vinylpyridine, Macromolecules. 34 (2001) 5376–5378. doi:10.1021/ma010440q.

[33] Y. Luo, D. Montarnal, S. Kim, W. Shi, K.P. Barteau, C.W. Pester, P.D. Hustad, M.D. Christianson, G.H. Fredrickson, E.J. Kramer, C.J. Hawker, Poly(dimethylsiloxane- b -methyl methacrylate): A Promising Candidate for Sub-10 nm Patterning, Macromolecules. 48 (2015) 3422–3430. doi:10.1021/acs.macromol.5b00518.

[34] F.A. Nicolescu, V.V. Jerca, I. Dancus, A. Petris, T.V. Nicolescu, I.B. Rau, V.I. Vlad, D.S. Vasilescu, D.M. Vuluga, Synthesis and characterization of side-chain maleimide-styrene copolymers with new pendant azobenzene moieties, J. Polym. Res. 18 (2011) 1009–1016. doi:10.1007/s10965-010-9501-6.

[35] A. Scarpaci, C. Cabanetos, E. Blart, V. Montembault, L. Fontaine, V. Rodriguez, F. Odobel, Postfunctionalization of poly(propargyl methacrylate) using copper catalyzed 1,3-dipolar Huisgen cycloaddition: An easy route to electro-optic materials, J. Polym. Sci. Part A Polym. Chem. 47 (2009) 5652–5660. doi:10.1002/pola.23606.

[36] K.A. Davis, K. Matyjaszewski, Atom Transfer Radical Polymerization of tert -Butyl Acrylate and Preparation of Block Copolymers, Macromolecules. 33 (2000) 4039–4047. doi:10.1021/ma991826s.

[37] K. Ishitake, K. Satoh, M. Kamigaito, Y. Okamoto, Stereospecific Free Radical and RAFT Polymerization of Bulky Silyl Methacrylates for Tacticity and Molecular Weight Controlled Poly(methacrylic acid), Macromolecules. 44 (2011) 9108–9117. doi:10.1021/ma202155b.

[38] J.M. Pelet, D. Putnam, High Molecular Weight Poly(methacrylic acid) with Narrow Polydispersity by RAFT Polymerization, Macromolecules. 42 (2009) 1494–1499. doi:10.1021/ma801433g.

[39] P.J. Miller, K. Matyjaszewski, Atom Transfer Radical Polymerization of (Meth)acrylates from Poly(dimethylsiloxane) Macroinitiators, Macromolecules. 32 (1999) 8760–8767. doi:10.1021/ma991077e.

[40] K. Matyjaszewski, D.A. Shipp, J.-L. Wang, T. Grimaud, T.E. Patten, Utilizing Halide Exchange To Improve Control of Atom Transfer Radical Polymerization, Macromolecules. 31 (1998) 6836–6840. doi:10.1021/ma980476r.

[41] S. Karanam, H. Goossens, B. Klumperman, P. Lemstra, "Controlled" Synthesis and Characterization of Model Methyl Methacrylate/tert-Butyl Methacrylate Triblock Copolymers via ATRP, Macromolecules. 36 (2003) 3051–3060. doi:10.1021/ma021399+.

[42] D.H. Grant, N. Grassie, The thermal decomposition of poly(t-butyl methacrylate), Polymer (Guildf). 1 (1960) 445–455. doi:10.1016/0032-3861(60)90060-4.

[43] G. Ducom, B. Laubie, A. Ohannessian, C. Chottier, P. Germain, V. Chatain, Hydrolysis of polydimethylsiloxane fluids in controlled aqueous solutions, Water Sci. Technol. 68 (2013). http://wst.iwaponline.com/content/68/4/813 (accessed July 24, 2017).

[44] M.F. Jung, M.A. Lyster, Quantitative dealkylation of alkyl esters via treatment with trimethylsilyl iodide. A new method for ester hydrolysis, J. Am. Chem. Soc. 99 (1977) 968–969. doi:10.1021/ja00445a062.

[45] G.A. Olah, S.C. Narang, Iodotrimethylsilane—a versatile synthetic reagent, Tetrahedron. 38 (1982) 2225–2277. doi:10.1016/0040-4020(82)87002-6.

[46] J.S. Moore, S.I. Stupp, Room temperature polyesterification, Macromolecules. 23 (1990) 65–70. doi:10.1021/ma00203a013.

[47] M. Cinar, A. Coruh, M. Karabacak, FT-IR, UV–vis, 1H and 13C NMR spectra and the equilibrium structure of organic dye molecule disperse red 1 acrylate: A combined

experimental and theoretical analysis, Spectrochim. Acta Part A Mol. Biomol. Spectrosc. 83 (2011) 561–569. doi:10.1016/j.saa.2011.09.003.

[48] J. Arias-Zapata, S. Böhme, J. Garnier, C. Girardot, A. Legrain, M. Zelsmann, Ultrafast Assembly of PS-PDMS Block Copolymers on 300 mm Wafers by Blending with Plasticizers, Adv. Funct. Mater. 26 (2016) 5690–5700. doi:10.1002/adfm.201601469.